Mg on Pd(111): The Formation of Local Order Observed by Photoelectron Diffraction

A. Fischer, R. Fasel, J. Osterwalder, A. Krozer, and L. Schlapbach
Physikalisches Institut der Universität Fribourg, CH-1700 Fribourg, Switzerland
(Received 20 May 1992)

We have studied the growth of Mg overlayers on Pd(111), a system with 16.6% misfit, by means of x-ray photoelectron diffraction. No long-range order is observed by low-energy electron diffraction. Pronounced forward-focusing maxima in Mg 1*s* emission indicate considerable short-range order. At coverages below 1 monolayer Mg is found to occupy fcc sites distributed over two layers. At higher coverages oriented clusters are formed, accommodating the misfit by alternatively occupying fcc and hcp sites. Comparison to single-scattering calculations suggests an average cluster size of less than 15 Å.

PACS numbers: 68.55.−a, 61.14.Rq

Metal-on-metal heteroepitaxy is by far less understood than the same phenomenon involving semiconductors, although its importance in the formation of, e.g., magnetic thin films or superlattices is well recognized [1]. The situation is here more complex due to a higher mobility of metal atoms at the interface and a strong tendency for intermixing. Investigations on systems with large misfits are particularly scarce because they normally lack long-range structural order.

We have studied the interface structure of Mg evaporated on Pd(111), motivated by our previous work on Mg hydride formation on such thin films using x-ray photoelectron spectroscopy (XPS) [2]. Pd has a face-centered-cubic (fcc) structure with a nearest-neighbor distance of 2.75 Å exposed on the (111) face. Mg is hexagonal close packed (hcp) with atoms 3.208 Å apart in the (0001) layers. The misfit is thus a very large 16.6%, and we were indeed not able to observe any long-range order by low-energy electron diffraction (LEED) for deposits between 0.3 and 5 monolayers (ML) on a cold substrate, implying that there is no order on a scale of 100 Å.

A suitable technique to probe the very short-range order, especially in ultrathin films, is x-ray photoelectron diffraction (XPD) [3]. In short, the angle-dependent photoelectron current is measured over a large part of the hemisphere above a single-crystal surface. The strong forward scattering of the photoelectrons along internuclear axes, and the short inelastic mean free path, makes the interpretation of such data particularly easy, and more subtle effects can be conveniently modeled using single-scattering cluster (SSC) calculations considering spherical-wave scattering [4,5]. If the films are less than 3 to 4 ML thick, multiple scattering plays only a minor role [6].

The experiments were performed in a modified Vacuum Generators ESCALAB Mark II Spectrometer, equipped with a three channeltron detection system and with a base pressure in the lower 10^{-11} mbar region. We used Si $K\alpha$ radiation ($h\omega = 1740$, $\Delta E \approx 1.2$ eV), which allowed us to measure the Mg 1*s* peak at $E_{\text{kin}} = 437$ eV with a high signal-to-background ratio.

The Pd(111) crystal was repeatedly sputtered and heated to 1000 K and then exposed several times to 10^{-6} mbar oxygen and reheated to 1000 K to remove carbon. To get a highly ordered surface we then annealed it at 1300 K for about 1 min and verified the crystalline order with LEED. The sample was then *in situ* transferred to a two-axis goniometer capable of sweeping the emission direction over the whole hemisphere above the surface by computer controlled crystal rotation. The data acquisition mode for obtaining 2π intensity maps has been described elsewhere [7]. The angular resolution was set to less than 3° full acceptance cone.

After scan times of up to 50 h less than 0.2 ML of oxygen was detected and the carbon contamination was below 0.02 ML. To reduce scan times we measured in most cases only one third of the hemisphere above the sample and completed the intensity maps exploiting the threefold symmetry of the crystal.

Mg was evaporated on the cooled sample ($T \leq 250$ K). Deposition on a hot Pd crystal (450 K) led to interdiffusion of Mg into the Pd, clearly visible in the XPD patterns. The evaporation rate was controlled with a quartz microbalance placed next to the sample. Calibration was made by XPS (Mg 1*s* and Pd 3*d*, respectively) using a layer-by-layer model. The large energy separation of the two peaks (437 and 1400 eV, respectively), the uncertainty of the inelastic mean free paths in such thin films, and likely deviations from layer-by-layer growth result in large error bars of the order of 20% for these values.

Figure 1 presents the measured 2π intensity maps of the Mg 1*s* peak at 437 eV kinetic energy for six different Mg coverages. The outer circles represent the 90° line, and data have been taken up to 78° polar angle. The intensities are represented in a linear gray scale.

At 0.3 ML coverage we already see a weak structure with a threefold symmetry, showing faint maxima near principal crystal axes [see Fig. 2(c)]. This is an indication for Mg being distributed in more than one layer, otherwise forward scattering occurs only within the surface layer itself, that is in grazing emission. A very similar behavior has been found for low coverages of Au on Cu(001) [8], a system which is known to form a two-dimensional surface alloy at submonolayer coverages.

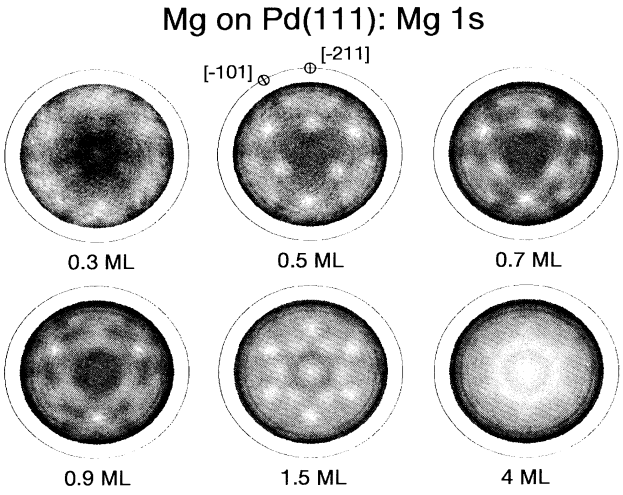

FIG. 1. Si $K\alpha$-excited Mg 1s (437 eV) intensity maps of Mg on Pd(111) in stereographic projection. Intensities are given in a linear gray scale with maximum intensities in white.

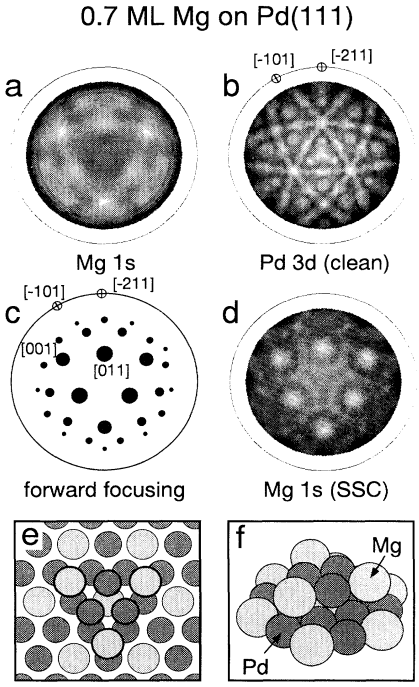

FIG. 2. Intensity maps of (a) Mg 1s emission from 0.7 ML Mg on Pd(111), (b) clean Pd(111), Pd 3d (1400 eV), (c) forward-focusing directions for a two-layer fcc (111) crystal, (d) SSC calculation for suggested cluster (see text). (e),(f) Mini-cluster with a Mg-seed layer in top view (e) and perspective view (f).

The relatively high overall anisotropy $(I_{max}-I_{min})/I_{max}$ of 50% is due to the instrumental $1/\cos\theta$ behavior typical for adsorbate emitters [8] and the intensity cutoff at higher angles which appears to be a consequence of inelastic losses inside the film [9].

A more pronounced structure is observed in the angular distribution maps of 0.5 and 0.7 ML. The anisotropy, which is here dominated by the pronounced forward-focusing peaks in the [001] and the [011] directions of the Pd crystal [see Fig. 2(c)] is 35% for the lower and 38% for the higher coverage, respectively.

In the 0.9 ML plot a beginning change from the threefold to a sixfold symmetry is observed. Obviously a rearrangement of atoms occurs. The [011] forward-scattering peaks [Fig. 2(c)] move further away from the normal, from polar angles near 35° to near 55°, indicating a displacement of the nearest-neighbor atoms from fcc to hcp adsorption sites. For the 1.5 ML sample this reconstruction is completed. We see a perfectly sixfold symmetry, an outer hexagon with three spots at the same [001] places as in the low-coverage samples and an inner hexagon rotated by 30°. A new forward-scattering peak is now visible along the surface normal. At 4 ML the outer hexagon is still faintly seen, while the inner hexagon is azimuthally smeared out, indicating increasing disorder.

We do not show here the corresponding Pd 3d and MVV Auger intensity maps which we measured simultaneously. They exhibit no major change in their structure with increasing coverage except for a general reduction of anisotropy. For Pd 3d it decreases for the [001] forward-focusing peak from 46% for the uncovered Pd(111) crystal to 22% for 1.8 ML Mg. Annealing the interface, however, leads to patterns with a sixfold symmetry, indicating ordered alloy formation.

The low-coverage patterns can be interpreted by a simple geometrical analysis. The comparison to the clean Pd(111) angular distribution map of Pd 3d (1400 eV) shown in Fig. 2(b) indicates that the structure of the substrate is continued in the overlayer. In the Mg 1s intensity map of the 0.7 ML sample [Fig. 2(a)] we see the same forward-focusing peaks along the [001] and the [011] directions with no significant shifts as compared to clean Pd, although more diffuse. This strongly suggests that the Mg atoms are distributed over two layers and continue the fcc stacking sequence of the crystal. To illustrate this more clearly, we give in Fig. 2(c) the positions of all forward-focusing peaks of a two-layer fcc (111) lattice. The peak anisotropies, indicated by the spot thickness, scale with the inverse distance between the emitter in the second layer and the scatterer. It is evident that this simple geometrical model reproduces most features seen in the experiment.

In order to learn more about the actual distribution of Mg atoms on this two-layer fcc lattice, the absolute peak anisotropies have to be considered. We performed SSC calculations [5] for different structural models. The experimental anisotropies agree best with those obtained from a model where Mg atoms form a seed layer in the top Pd layer [see Fig. 2(e)]. Approximately every fourth Pd atom in this layer is replaced by a Mg atom. The

larger Mg atoms can be accommodated quite well due to alloying effects. In fact, the resulting Mg-Pd distance of 2.75 Å is close to its value in an ordered MgPd alloy (2.736 Å) [10]. However, a fcc overlayer which is completely ordered on the length scale of XPD (10–15 Å at this photoelectron energy) on top of this layer did not give the best results, because the spots in the [001] directions were highly overemphasized. In contrast a local cluster of six atoms around the seed-layer Mg [see Figs. 2(e) and 2(f)] improved the agreement. The important point here is not the size or the shape of the cluster, but that not all seed-layer Mg atoms have all six [011] and [001] type nearest neighbors present in the top layer. The best agreement was achieved by an incoherent superposition of calculations for the small cluster [Fig. 2(e)] with 50% weight and for the fully ordered double layer with 50%, shown in Fig. 2(d).

The calculations could not significantly distinguish between Mg and Pd scatterers, and one can only use chemical intuition to speculate on the composition and occupation of the top layer. Using a rigid sphere model with alloy atomic radii, one obtains the best agreement of the forward-focusing peak positions with experiment for the model depicted in Fig. 2(e). The formation of the mixed seed layer releases Pd atoms into the new top layer, a process similar to that observed in Au/Cu(001) [8].

In the 1.5 ML sample not only fcc sites are occupied, but hcp sites as well, according to the three additional forward-scattering peaks in the outer hexagon, which also indicate that these hcp sites are grouped around Mg seed atoms. The interpretation of the inner hexagon, rotated by 30° with respect to the outer one, is less obvious. A simple switching from fcc to hcp stacking does not produce the observed emission pattern [11]. Islands of Mg atoms arranged in a regular hcp stacking sequence cannot explain the rotation of the inner hexagon [see Fig. 3(c)]. After considering various configurations we found the by far best agreement for the local cluster formation around Mg seed atoms shown in Figs. 3(e) and 3(f). As indicated in Fig. 3(f), these clusters contain the forward-focusing directions that account for the inner and outer hexagons as well as for the normal-emission peak.

Figure 4 illustrates a likely reaction path for the formation of this local configuration. As evidenced by the forward-focusing peaks, the three atoms nearest to a Mg seed atom switch from fcc into hcp sites, giving room for an additional atom in the center atop position. This is only possible if the top layer is not complete, consistent with our model for the low coverages. The atop bonded atom gives rise to the focusing peak along the normal. Furthermore, the distance between hcp and fcc sites on Pd(111) (3.176 Å) is very close to the nearest-neighbor

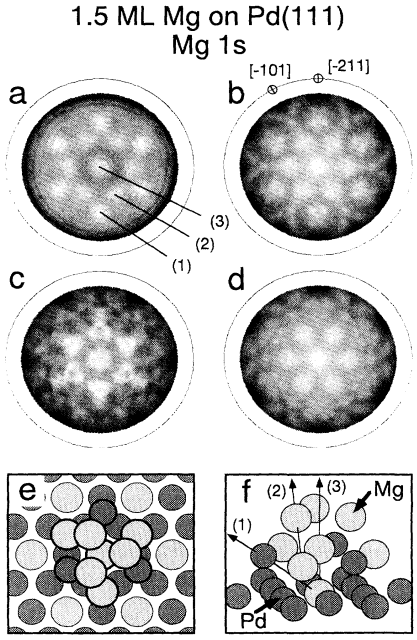

FIG. 3. Angular distribution maps of Mg 1*s* emission from 1.5 ML Mg on Pd(111): (a) experiment; SSC calculations for (b) suggested reconstructed cluster (see text), (c) 3 ML of hexagonal Mg on Pd(111), (d) "long-range" ordered cluster; (e) top view and (f) perspective view of reconstructed local cluster geometry. Important forward-focusing directions are indicated and labeled, with corresponding labels appearing in (a). Polar angles are 55° (1), 35° (2), and 0° (3).

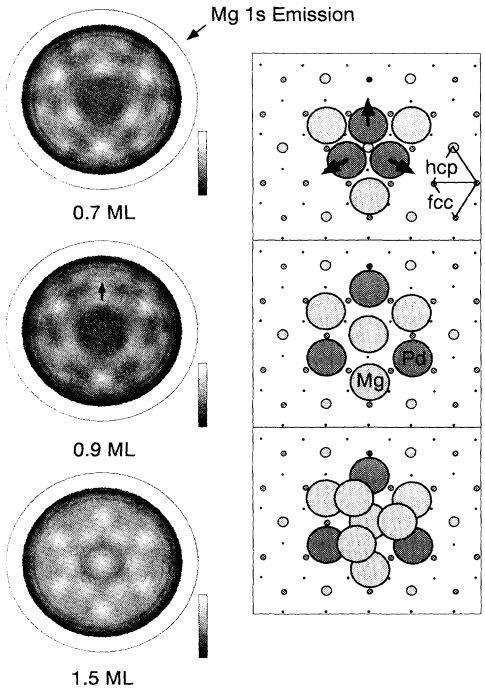

FIG. 4. Illustration of atomic rearrangements as observed by Mg 1*s* forward focusing. For better visibility atomic radii are reduced to 80%. Underlying layers are shown with strongly reduced radii.

distance in bulk Mg (3.208 Å). Within these local clusters the misfit is thus reduced from 16.6% to 1%. Three further Mg atoms can occupy six equivalent sites on top of this hexagon, forming two domains and producing the inner hexagon in the intensity maps.

As for the low coverage phase, these forward-focusing arguments can only provide information on atomic positions, while SSC simulations are needed to learn more about site occupation in the reconstructed layers. Diffraction patterns for more than twenty different cluster models have been calculated. Also in this case, a fully occupied second layer which is ordered on the scale of 10–15 Å is incompatible with our data as shown by the simulated pattern in Fig. 3(d). We obtained the best agreement by taking a one-to-one superposition of the "long-range" ordered structure and a local cluster consisting of seven seed Mg and a pyramid of ten atoms around the seed in the center, arranged in the way shown in Figs. 3(e) and 3(f). The calculated intensity map is displayed in Fig. 3(b). Again we emphasize that we cannot determine exact cluster sizes and shapes but rather obtain statistical information on site occupation in the short range.

Because of its very low coherence length XPD is a suitable method to investigate very local ordering, even in samples that show no long-range order on a scale > 100 Å as seen by LEED. We have shown that Mg deposited on Pd(111) at about 250 K forms a mixed seed layer replacing Pd atoms in the outermost Pd layer. For low coverages these released Pd atoms, together with extra Mg atoms, adsorb on fcc sites only, forming local clusters around Mg seed atoms. They locally continue the bulk fcc lattice up to a critical density between 0.7 and 0.9 ML. The average size of these ordered clusters, which may not be uniform, is below the length scale of XPD, which in this case is 10–15 Å. At higher coverages, some top-layer atoms switch to hcp sites, providing room for on-top adsorption on the Mg seeds. The hexagons thus formed serve as templates to accommodate a next layer of Mg with almost no misfit and with a rotation of the hexagonal symmetry by 30° relative to that of the substrate. This unusual way of accommodating 16.6% misfit represents a novel form of pseudoepitaxy for a metal-metal system.

This work has been supported by the Schweizerischer Energieforschungs Fonds and by the Schweizerischer Nationalfonds.

[1] A. S. Arrott, B. Heinrich, C. Liu, and S. T. Purcell, in *Thin Films Growth Techniques for Low-Dimensional Structures*, edited by R. F. C. Farrow, S. S. P. Parkin, P. J. Dobsow, J. H. Neuve, and A. S. Arrott (Plenum, New York, 1987).

[2] A. Fischer, H. Kösler, and L. Schlapbach, J. Less-Common Met. **103**, 808 (1991); A. Fischer, A. Krozer, and L. Schlapbach, Surf. Sci. (to be published).

[3] C. S. Fadley, in *Synchrotron Radiation Research: Advances in Surfaces Science*, edited by R. Z. Bachnach (Plenum, New York, 1989); W. F. Egelhoff, Jr., Crit. Rev. Solid State Mater. Sci. **16**, 213 (1990); S. A. Chambers, Adv. Phys. **40**, 357 (1991).

[4] J. J. Rehr and R. C. Albers, Phys. Rev. B **41**, 8139 (1990).

[5] D. J. Friedman and C. S. Fadley, J. Electron Spectrosc. Relat. Phenom. **51**, 689 (1990).

[6] A. Kaduwela, G. S. Herman, D. J. Friedman, and C. S. Fadley, Phys. Scr. **41**, 948 (1990).

[7] J. Osterwalder, T. Greber, A. Stuck, and L. Schlapbach, Phys. Rev. B **44**, 13764 (1991).

[8] D. Naumovic, A. Stuck, T. Greber, J. Osterwalder, and L. Schlapbach, Surf. Sci. **269**, 719 (1992); **277**, 235 (1992).

[9] R. Fasel (unpublished).

[10] R. Ferro, J. Less-Common Met. **1**, 424 (1959).

[11] C. M. Wei, T. C. Zhao, and S. Y. Tong, Phys. Rev. Lett. **65**, 2278 (1990).

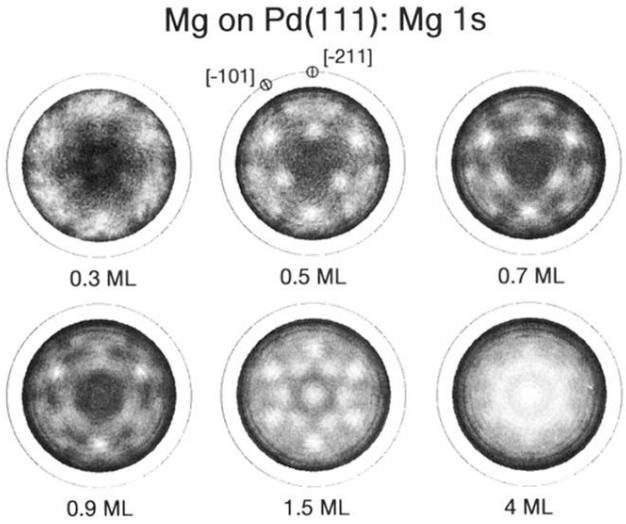

FIG. 1. Si $K\alpha$-excited Mg 1s (437 eV) intensity maps of Mg on Pd(111) in stereographic projection. Intensities are given in a linear gray scale with maximum intensities in white.

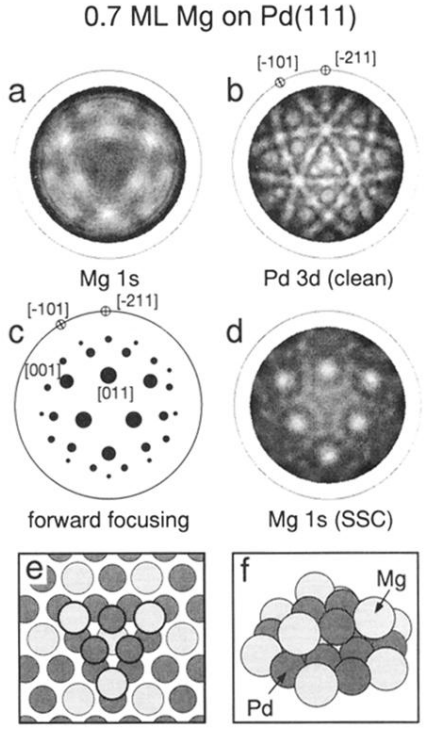

FIG. 2. Intensity maps of (a) Mg 1*s* emission from 0.7 ML Mg on Pd(111), (b) clean Pd(111), Pd 3*d* (1400 eV), (c) forward-focusing directions for a two-layer fcc (111) crystal, (d) SSC calculation for suggested cluster (see text). (e),(f) Mini-cluster with a Mg-seed layer in top view (e) and perspective view (f).

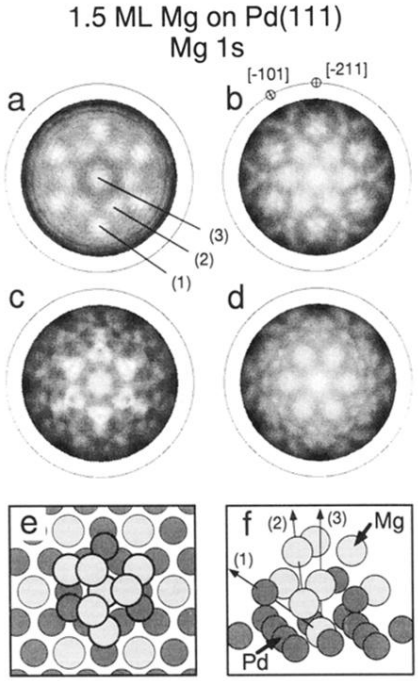

FIG. 3. Angular distribution maps of Mg 1*s* emission from 1.5 ML Mg on Pd(111): (a) experiment; SSC calculations for (b) suggested reconstructed cluster (see text), (c) 3 ML of hexagonal Mg on Pd(111), (d) "long-range" ordered cluster; (e) top view and (f) perspective view of reconstructed local cluster geometry. Important forward-focusing directions are indicated and labeled, with corresponding labels appearing in (a). Polar angles are 55° (1), 35° (2), and 0° (3).

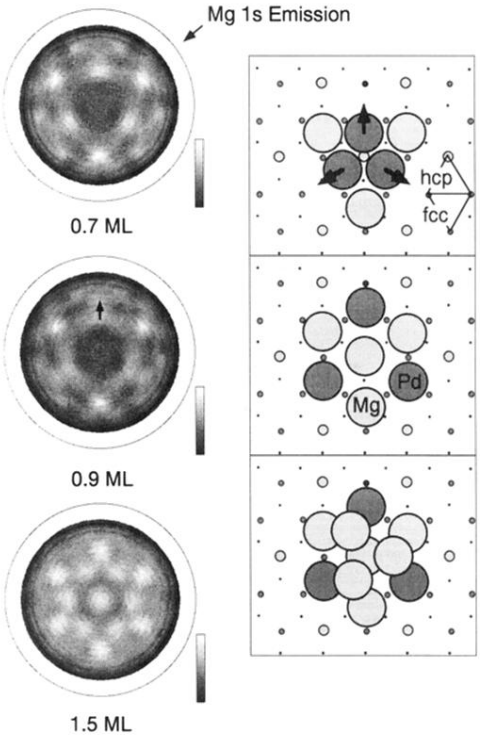

FIG. 4. Illustration of atomic rearrangements as observed by Mg 1*s* forward focusing. For better visibility atomic radii are reduced to 80%. Underlying layers are shown with strongly reduced radii.